regenerate surface hydroxyl groups or to react with the {Si}–O–Rh(allyl)$_2$ groups to eliminate allyls as propene and to generate Rh(III) ions, which are reduced to zerovalent rhodium, which migrates over the surface and aggregates to form metal particles.

A schematic representation of the surface organometallic chemistry is shown in Figure 8. This picture is consistent with (1) the observation that CO inhibited the reaction with H_2 at 25 °C, (2) the observation of D_2 exchange with the hydroxyl groups of the support, (3) production of propene and propane upon reaction with H_2, (4) electronic considerations regarding the rhodium center, and (5) the observation of rhodium metal formation. The key is that a separate rhodium species acts as the site for H_2 activation, which leads to the ready formation of rhodium metal from {Si}–O–Rh(allyl)$_2$ groups.

Genesis of Catalytically Active Species. The ease with which {Si}–O–Rh(allyl)$_2$ is reduced in the presence of H_2 to give rhodium metal led us to suspect that rhodium metal, and not a complex related to {Si}–O–Rh(allyl)$_2$, might have been the catalyst in the reported hydrogenations of alkenes and arenes.[2b,c] If rhodium metal were the actual catalyst, one would expect an induction period followed by a rise in catalytic activity as rhodium metal formed from the diallyl complex. Consistent with this expectation, results of the catalytic hydrogenation experiment carried out in the flow reactor (Figure 9) show that a short induction period was followed by a rapid rise in the conversion of toluene to methylcyclohexane. Subsequent treatment of the catalyst with helium for 10 h and resumption of flow of toluene and H_2 led to 100% conversion of the toluene. The used catalyst was black. All these results are consistent with the reduction of the {Si}–O–Rh(allyl)$_2$ to rhodium metal, which we infer to be the catalytically active species. The interpretation is consistent with the results of Ward and Schwartz, who found that the olefin hydrogenation was first order in H_2 and zero order in olefin; these are the dependencies expected for a rhodium metal catalyst.[26,27]

Acknowledgment. We thank R. P. Eischens and E. D. Nicholson for helpful discussions and K. E. Foley for preparation of microscopy samples. This research was supported by the National Science Foundation.

Registry No. Rh(allyl)$_3$, 12082-48-3; CO, 630-08-0; H_2, 1333-74-0; HCl, 7647-01-0; toluene, 108-88-3.

---

(26) Bond, G. C.; Phillipson, J. J.; Wells, P. B.; Winterbottom, J. M. *Trans. Faraday Soc.* **1966**, *62*, 281.

(27) Graydon, W. F.; Langan, M. D. *J. Catal.* **1981**, *69*, 180. Rhodium aggregates smaller than 12 Å in diameter apparently have low catalytic activity for benzene hydrogenation, whereas aggregates having diameters between 12 and 20 Å have higher activity.

A Molecular Orbital Calculation of the $[Re_2Cl_8]^{2-}$ Ion by the Relativistic SCF-Xα-SW Method. Redetermination and Reassignment of the Electronic Absorption Spectrum

Bruce E. Bursten, F. Albert Cotton,* Phillip E. Fanwick, and George G. Stanley

Contribution from the Department of Chemistry, Texas A&M University, College Station, Texas 77843. *Received July 1, 1982*

Abstract: The electronic structure and spectrum of the $[Re_2Cl_8]^{2-}$ ion have been reinvestigated. A new calculation by the SCF-Xα-SW method gives results in essential agreement with the earlier calculation of Mortola et al., but the inclusion of corrections for inner-shell and valence relativistic effects causes appreciable shifts that are important in analyzing the spectrum. The polarized single-crystal spectrum has been remeasured under more defined conditions and better resolution, and the new results reveal several minor and one major flaw in the earlier measurements. The new computational and experimental data lead us to revise the previously proposed assignments of the weak, forbidden bands lying between the $\delta \rightarrow \delta^*$ transition and the strong near-UV absorptions.

The $[Re_2Cl_8]^{2-}$ ion occupies a unique place in the development of our understanding of multiple bonds between metal atoms since it was the first well-defined example of such bonding between a discrete pair of metal atoms, as well as the first example of a quadruple bond of any kind, and it remains the prototypal species in this now large field of chemistry. It is thus a matter of more than casual interest to have a thorough understanding of the electronic structure of this particular ion.

Both $[Re_2Cl_8]^{2-}$ and the isostructural and isoelectronic $[Mo_2Cl_8]^{4-}$ ions have been the subjects of some of the first rigorous MO calculations[1,2] carried out on quadruply bonded species, in each case by the SCF-Xα-SW method. While the published results for $[Mo_2Cl_8]^{4-}$ appear to be as reliable as possible within the scope of the method and have been fully reported, this is not entirely the case for the $[Re_2Cl_8]^{2-}$ ion. For one thing, the results of the original calculation[1] have never been presented in full, and because of the tragic death of the senior investigator, A. P. Mortola, probably never can be. Second, for $[Re_2Cl_8]^{2-}$, as for all compounds containing atoms of such high atomic number as rhenium, valence corrections for relativistic effects, which can amount to an electron volt, should (and now can) be made in order to justify considering the results as final.

It is our purpose here to present the results in detail for what we believe to be the definitive SCF-Xα-SW calculation, including relativistic effects, on the $[Re_2Cl_8]^{2-}$ ion and to use these results together with much new spectroscopic data to reexamine the assignments previously proposed by Trogler, Cowman, Gray, and Cotton[3] (hereafter cited as TCGC) for the spectral region between the $\delta \rightarrow \delta^*$ transition at about 14 200 cm^{-1} and the first strong

---

(1) Mortola, A. P.; Moskowitz, J. W.; Rösch, N. *Int. J. Quantum Chem., Symp.* **1974**, *No. 8*, 161. Mortola, A. P.; Moskowitz, J. W.; Rösch, N.; Cowman, C. D.; Gray, H. B. *Chem. Phys. Lett.* **1975**, *32*, 283.

(2) (a) Norman, J. G., Jr.; Kolari, H. J. *J. Chem. Soc., Chem. Commun.* **1974**, 303; *J. Am. Chem. Soc.* **1975**, *97*, 33. (b) Noodleman, L.; Norman, J. G., Jr. *J. Chem. Phys.* **1979**, *70*, 4903.

(3) Trogler, W. C.; Cowman, C. D.; Gray, H. B.; Cotton, F. A. *J. Am. Chem. Soc.* **1977**, *99*, 2993.

0002-7863/83/1505-3082\$01.50/0

Table I. Structural and Calculational Parameters Used for $[Re_2Cl_8]^{2-}$ under D_{4h} Symmetry[a]

atom	sphere radius, Å	α values
outer sphere	4.098	0.71723
Re	1.360	0.69316
Cl	1.298	0.72325

[a] Re–Re 2.224 Å; Re–Cl 2.320 Å; Re–Re–Cl 104.0°.

absorption band at about 27 000 cm^{-1}.

This work proceeded through the interplay of experimental and theoretical studies, The first results of the new calculation led us to have some misgivings about the spectra and assignments in TCGC. We therefore decided to remeasure the crystal spectra. By combining the new computational with the new experimental results we have arrived at a new and independent analysis of the spectrum. Some of our conclusions are in harmony with the earlier ones while others are not. Some of the differences arise from changes in the computational results while others have their origin in differences between our new experimental observations and those previously measured elsewhere. The manifest superiority of both the present calculation and the present experimental measurements makes the new assignments more credible than those of TCGC.

Computational and Experimental Procedures

Initial Parameters. Coordinates for $[Re_2Cl_8]^{2-}$ were taken from the crystal structure of $[N\text{-}n\text{-}Bu_4]_2[Re_2Cl_8]$[4] and idealized to D_{4h} symmetry. An initial molecular charge density and potential were constructed from a superposition of Herman–Skillman atomic charge densities[5] for Re^+ and $Cl^{0.5-}$. The α exchange parameters for Cl and Re were taken from (Cl), or extrapolated from (Re), the tabulations of Schwarz;[6] a valence-weighted average of these was used for the extramolecular and interatomic regions. Overlapping atomic sphere radii[7] were taken as 89% of the atomic number radii, in accordance with the nonempirical procedure of Norman.[8] The outer sphere was made tangential to the outermost atomic spheres. Structural and computational parameters are summarized in Table I.

Nonrelativistic Calculation. The basis set used in the calculation consisted of partial waves through $l = 7$, $l = 3$, and $l = 2$ on the outer, Re, and Cl spheres, respectively. A Watson sphere[9] with a charge of 2+ and a radius of 8.744 31 au was used to simulate the stabilizing influence of a surrounding ionic lattice. Core levels (Re: 1s, 2s, 2p, 3s, 3p, 3d, 4s, 4p, 4d, 4f, 5s, 5p; Cl: 1s, 2s, 2p) were calculated explicitly by using only the potential within the sphere surrounding the atom in question.

The iteration to self-consistency was begun with a 19:1 average of the initial and final potentials. This ratio was gradually changed to 17:3 as the calculation neared convergence. After 41 iterations the largest change at any point in the potential was <0.0005 hartree (0.01 eV) and the calculation was considered converged. The virial ratio ($=2T/V$) at convergence was 1.0007. Each iteration required ca. 30 s of cpu time on an Amdahl 470/V6 computer.

Relativistic Calculation. The converged nonrelativistic potential was used as the starting potential for the relativistic calculation. The formalism of Wood and Boring[10] was used to incorporate the relativistic effects, requiring modification of only the diagonal (one-center) terms of the secular matrix. The Re core levels and all valence levels explicitly included these effects, which were slowly mixed into the potential over 10 iterations. A total of 28 iterations were required to converge the relativistic calculation, each iteration requiring ca. 3 s more cpu time than for the nonrelativistic calculation. The virial ratio at convergence increased to 1.0428 as a consequence of the relativistic formalism.

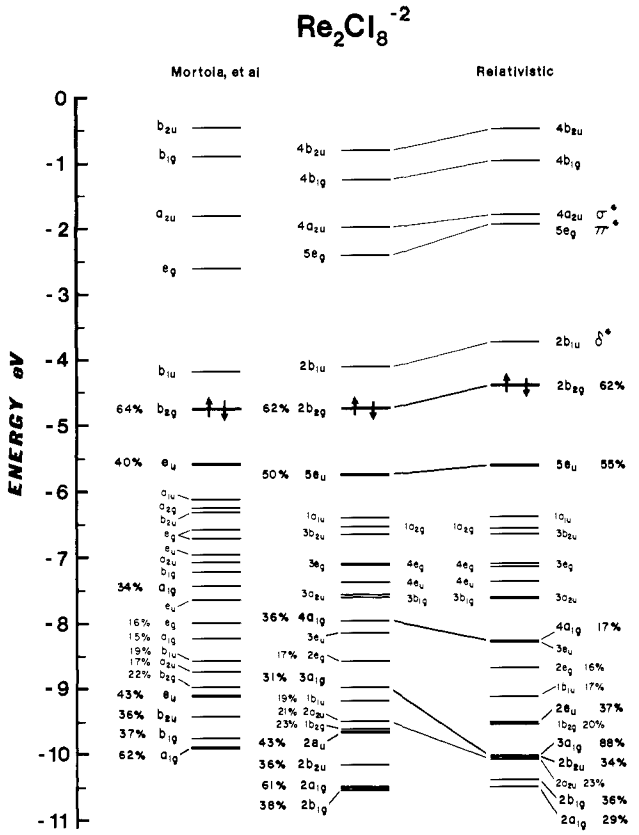

Figure 1. Results of the present SCF-Xα-SW calculations, both relativistic and nonrelativistic, with the nonrelativistic results of Mortola et al.[1] shown for comparison.

Transition Energies. The converged relativistic ground-state potential was used to search for virtual levels below -0.015 hartree. The energies of several electronic transitions were calculated by using Slater's transition-state formalism. Transition-state calculations were performed with both spin-restricted and spin-unrestricted potentials, yielding the multiplet-averaged transition energy and the triplet transition energy, respectively; from these the spin-allowed singlet to singlet transition energies were deduced.[11] Several other transition energies were estimated by assuming that orbitals of similar energy and character would exhibit nearly the same relaxation upon excitation.

Crystal Spectra. $[N\text{-}n\text{-}Bu_4]_2[Re_2Cl_8]$ was prepared by the standard literature method.[12] Large well-formed crystals were obtained by slow evaporation of a solution of the compound in a 1:1 mixture of 12 M HCl/CH_3OH. The crystals selected for investigation were parallelepipeds with one large, nonrectangular face. One such crystal was mounted on a fiber and indexed on a Syntex P$\bar{1}$ diffractometer. The cell parameters were found to be in satisfactory agreement with those reported in the crystal structure determination.[4] The crystal was then mounted on a Huber 301 optical goniometer, and it was determined that the

---

(4) Cotton, F. A.; Frenz, B. A.; Stults, B. R.; Webb, T. R. *J. Am. Chem. Soc.* **1976**, *98*, 2768.

(5) Herman, F.; Skillman, S. "Atomic Structure Calculations"; Prentice-Hall: Englewood Cliffs, NJ, 1963.

(6) (a) Schwarz, K. *Phys. Rev. B* **1972**, *5*, 2466. (b) Schwarz, K. *Theor. Chim. Acta* **1974**, *34*, 225.

(7) Herman, F.; Williams, A. R.; Johnson, K. H. *J. Chem. Phys.* **1974**, *61*, 3508.

(8) Norman, J. G., Jr. *Mol. Phys.* **1976**, *31*, 1191.

(9) Watson, R. E. *Phys. Rev.* **1958**, *111*, 1108.

(10) Wood, J. H.; Boring, M. A. *Phys. Rev. B* **1978**, *18*, 2701.

(11) The transition-state formalism and derivation of the singlet–triplet splittings is described in: Slater, J. C. "Quantum Theory of Molecules and Solids. The Self-Consistent Field for Molecules and Solids"; McGraw-Hill: New York, 1974; Vol. 4. We are grateful to one of the referees for pointing out that our procedure for calculating the singlet–triplet splittings is not the only one available (see: Bagus, P. S.; Bennett, B. I. *Int. J. Quantum Chem.* **1975**, *9*, 143. Zeigler, T.; Rank, A.; Baerends, E. J. *Theor. Chim. Acta*, **1977**, *43*, 261).

(12) Cotton, F. A.; Curtis, N. F.; Johnson, B. F. G.; Robinson, W. R. *Inorg. Chem.* **1965**, *4*, 326.

Table II. Upper Valence Molecular Orbitals of $[Re_2Cl_8]^{2-}$

level	energy, eV	% contributions[b] Re	Cl	int	out	Re angular contributions
		A. Nonrelativistic Calculation				
$5a_{1g}$	−0.733	1	4	32	63	
$4b_{2u}$	−0.791	45	40	4	11	100% d
$4b_{1g}$	−1.244	42	39	6	12	98% d, 2% f
$4a_{2u}$	−1.970	60	19	18	3	9% p, 88% d, 2% f
$5e_g$	−2.387	72	19	7	1	98% d, 2% f
$2b_{1u}$	−4.113	66	22	10	2	100% d
$2b_{2g}$[a]	−4.728	61	25	13	2	100% d
$5e_u$	−5.728	50	46	0	3	8% p, 89% d, 2% f
$1a_{1u}$	−6.377	0	87	11	1	
$1a_{2g}$	−6.534	0	85	13	1	
$3b_{2u}$	−6.635	0	87	11	2	
$4e_g$	−7.077	4	83	11	3	
$3e_g$	−7.095	4	81	13	2	
$4e_u$	−7.368	5	78	14	3	
$3a_{2u}$	−7.558	5	78	14	3	
$3b_{1g}$	−7.597	1	80	18	1	
$4a_{1g}$	−7.941	36	50	12	2	23% s, 15% p, 60% d, 1% f
$3e_u$	−8.134	6	76	15	3	
$2e_g$	−8.568	17	72	9	2	29% p, 70% d, 1% f
$3a_{1g}$	−8.963	31	57	10	1	51% s, 41% d, 7% f
$1b_{1u}$	−9.167	19	62	18	1	99% d, 1% f
$2a_{2u}$	−9.485	21	74	2	3	48% s, 2% p, 47% d, 3% f
$1b_{2g}$	−9.597	23	56	20	1	100% d
$2e_u$	−9.642	43	45	11	1	1% p, 98% d, 1% f
$2b_{2u}$	−10.155	36	62	0	2	98% d, 2% f
$2a_{1g}$	−10.501	61	38	0	1	4% p, 94% d, 2% f
$2b_{1g}$	−10.503	38	61	0	2	100% d
		B. Relativistic Calculation				
$4b_{2u}$	−0.476	45	38	4	12	100% d
$5a_{1g}$	−0.725	1	4	32	64	
$4b_{1g}$	−0.959	42	37	6	14	99% d, 1% f
$4a_{2u}$	−1.780	58	18	20	3	11% p, 87% d, 2% f
$5e_g$	−1.923	73	18	7	1	98% d, 2% f
$2b_{1u}$	−3.714	67	21	10	2	100% d
$2b_{2g}$[a]	−4.374	62	23	13	2	100% d
$5e_u$	−5.588	55	41	0	4	8% p, 90% d, 2% f
$1a_{1u}$	−6.372	0	87	11	1	
$1a_{2g}$	−6.530	0	85	13	1	
$3b_{2u}$	−6.629	0	87	11	2	
$4e_g$	−7.069	4	81	14	1	
$3e_g$	−7.122	3	83	10	3	
$4e_u$	−7.356	5	79	14	2	
$3a_{2u}$	−7.582	5	74	18	2	
$3b_{1g}$	−7.591	1	80	18	1	
$4a_{1g}$	−8.265	17	63	19	1	14% s, 35% p, 51% d
$3e_u$	−8.277	7	75	15	3	
$2e_g$	−8.663	16	74	8	2	56% p, 63% d, 1% f
$1b_{1u}$	−9.089	17	64	18	1	99% d, 1% f
$2e_u$	−9.479	37	50	11	1	1% p, 97% d, 1% f
$1b_{2g}$	−9.502	20	58	21	1	100% d
$3a_{1g}$	−9.978	88	12	0	0	27% s, 5% p, 67% d, 4% f
$2b_{2u}$	−10.002	34	64	0	2	98% d, 2% f
$2a_{2u}$	−10.040	23	72	2	2	60% s, 3% p, 35% d, 2% f
$2b_{1g}$	−10.350	36	62	0	2	100% d
$2a_{1g}$	−10.461	29	66	3	2	36% s, 2% p, 62% d

[a] Highest occupied molecular orbital. [b] Int and out refer to the percent contributions from the inter sphere region and outside of the outer sphere, respectively.

Table III. Calculated Energies for the Singlet and Triplet Electronic Transitions of $[Re_2Cl_8]^{2-}$ below 30 000 cm^{-1} [a]

transition	type	state[b]	transition energy, cm^{-1} singlet	triplet
$2b_{2g} \rightarrow 2b_{1u}$	$\delta \rightarrow \delta^*$	A_{2u}	7040	3650
$5e_u \rightarrow 2b_{1u}$	$\pi \rightarrow \delta^*$	E_g	16 730	14 020
$2b_{2g} \rightarrow 5e_g$	$\delta \rightarrow \pi^*$	E_g	22 120	18 130
$1a_{1u} \rightarrow 2b_{1u}$	LMCT	B_{1g}	24 050	23 280
$1a_{2g} \rightarrow 2b_{1u}$	LMCT	B_{2u}	(25 330)	(24 540)
$3b_{2u} \rightarrow 2b_{1u}$	LMCT	A_{2g}	(26 030)	(25 330)
$4e_g \rightarrow 2b_{1u}$	LMCT	E_u	29 500	28 770
$3e_g \rightarrow 2b_{1u}$	LMCT	E_u	(29 960)	(29 230)
$5e_u \rightarrow 5e_g$	$\pi \rightarrow \pi^*$	A_{2u}	31 470	28 550

[a] Values in parentheses are estimated from shifts of similar transitions. All other transition energies are calculated using Slater's transition state formalism. [b] The ground state is $^1A_{1g}$. Orbitally allowed transitions are to A_{2u} and E_u states.

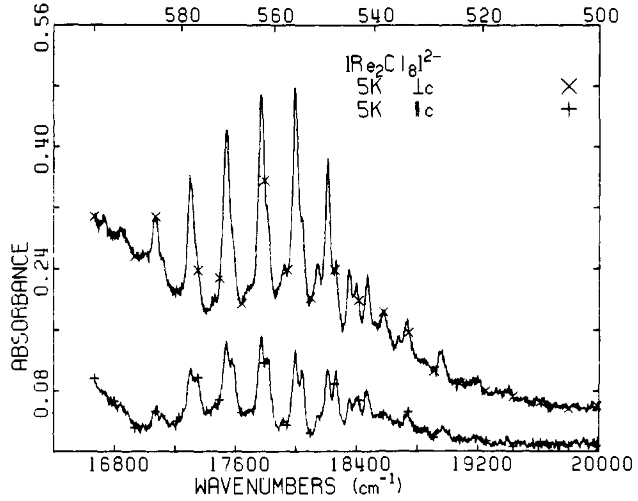

Figure 2. Crystal spectrum of $[N(C_4H_9)_4]_2[Re_2Cl_8]$ in the range 500–600 nm, recorded at 5 K. Every fifth data point collected in the ⊥*c* (×) and ∥*c* (+) polarizations is given.

large face was the (110) face with the *c* axis oriented along the shorter of the two diagonals. For a monoclinic crystal the extinction directions are required to be parallel and perpendicular to the *c* axis for this face.

Spectra were recorded on a Cary 17D spectrophotometer, using equipment previously described.[13] Two Glan-Thompson polarizers were used, one behind the sample and the other in the reference beam. Each crystal was mounted over a slit made in a brass foil plate. A very small amount of silicone grease was used to hold the crystal in place, and care was taken to avoid getting grease in the slit. The plate was mounted with the slit vertical in a sample holder attached to a brass rod that fits into the cryostat. The spectra of several crystals were recorded, and good reproducibility of band positions and relative intensities was found.

Results

Xα-SW Calculations. As can be clearly seen in Figure 1 the nonrelativistic Xα-SW calculations reported here differ only slightly from those previously reported by Mortola et al.,[1] the minor differences arising from the choice of sphere radii. The results of our nonrelativistic and relativistic calculations are compared in Figure 1 and Table II for the lowest virtual orbitals and the filled valence shell orbitals. The relativistic corrections cause large energy shifts in the Re core levels and smaller shifts to valence orbitals containing significant Re character, while, as expected, the primarily chlorine-based MO's are scarcely affected. The observed differential shifts are similar in magnitude and direction to those observed in atomic calculations using this and other relativistic formalisms[15] and to previous molecular calculations performed in these laboratories.[16,17]

Because the relativistically induced shifts in rhenium-containing valence orbitals are not uniform, the inclusion of relativistic

---

(13) Cotton, F. A.; Fanwick, P. E. *J. Am. Chem. Soc.* **1979**, *101*, 5252.

(14) Cotton, F. A. *J. Mol. Struc.* **1980**, *59*, 97. Cotton, F. A.; Walton, R. A. "Multiple Bonds Between Metal Atoms"; Wiley: New York 1982.

(15) For an excellent recent review of the Xα mehtod including an extensive discussion of relativistic Xα calculations, see: Case, D. A. *Annu. Rev. Phys. Chem.* **1982**, *33*, 151.

(16) Bursten, B. E.; Cotton, F. A.; Green, J. C.; Seddon, E. A.; Stanley, G. G. *J. Am. Chem. Soc.* **1980**, *102*, 955.

(17) Cotton, F. A.; Hubbard, J. L.; Lichtenberger, D. L.; Shim, I. *J. Am. Chem. Soc.* **1982**, *104*, 679.

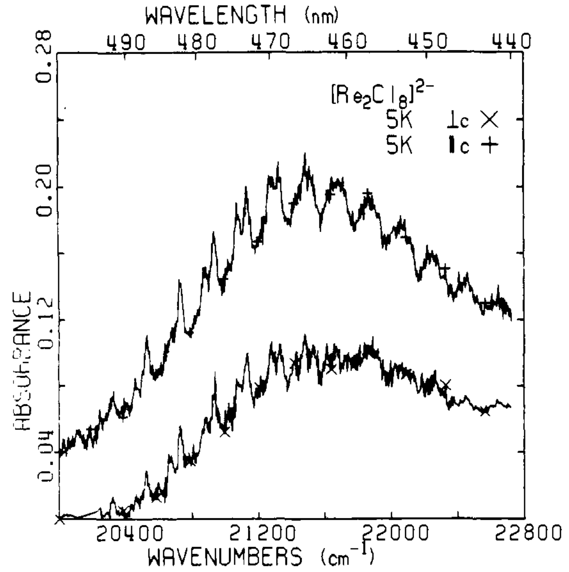

Figure 3. Crystal spectrum of $[N_4(C_9H_4)]_2[Re_2Cl_8]$ in the range 440–500 nm, recorded at 5 K. Use of × and + for data as in Figure 2.

corrections has a profound effect upon calculated electronic transition energies. Pertinent calculated singlet and triplet transitions are reported in Table III. No attempt has been made to calculate explicitly the spin–orbit splittings for orbitally degenerate triplet states.

Crystal Spectroscopy. Computer-plotted spectra for the two regions of interest, 16 200–20 000 and 20 000–22 000 cm^{-1}, are presented in Figures 2 and 3. Peak positions for vibrational fine structure, progressional assignments, and spacings are tabulated in Table IV. Theoretical polarization ratios ($\perp c/\parallel c$) for the (110) face as calculated from the crystal structure, with proper account taken of the disorder, are 2.31 and 0.64 for z- and xy-polarized transitions, respectively.

Discussion

It is generally agreed that the first electronic transition observed for $[Re_2Cl_8]^{2-}$, a progression with its origin at about 14 200 cm^{-1} corresponds to the $\delta \rightarrow \delta^*$ ($^1A_{2u} \leftarrow {}^1A_{1g}$) allowed transition,[18] and we concur in this assignment. It may be noted that even with the inclusion of relativistic corrections the transition energy calculated by the SCF-Xα-SW method is low by about a factor of 2. This discrepancy is undoubtedly due to the inadequacy of any molecular orbital description for weakly coupled electrons[14] and would most likely be mitigated by use of the valence-bond Xα formalism developed by Noodleman and Norman and successfully applied to the $[Mo_2Cl_8]^{4-}$ case. It is interesting that a recent multiconfiguration valence bond calculation by Hay[19] using a relativistic effective core potential overestimates the energy of this transition by more than 8000 cm^{-1}. This result may be attributed to the inherent tendency of valence bond theory to underestimate the amount of interaction between the electrons comprising the δ bond. In any case, spectroscopic evidence firmly supports the $\delta \rightarrow \delta^*$ assignment, and we need not discuss this band further.

Definitive assignments for the remainder of the spectrum remain to be achieved, however. In the previous report of TCGC,[3] the following proposals were made. For the weak absorption centered around 566 nm, band I, a vibrational progression with a frequency of ~230 cm^{-1} was observed and the band was assigned to a spin-allowed, orbitally forbidden $\delta \rightarrow \pi^*$ ($^1E_g \leftarrow {}^1A_{1g}$) transition. For an absorption centered at about 478 nm, band II, the

Table IV. Observed Transitions between 600 and 440 nm in the 5 K Spectrum of $[N\text{-}n\text{-}Bu_4]_2[Re_2Cl_8]$[a]

assignment	λ, nm	$\bar{\nu}$, cm^{-1}	$\Delta\bar{\nu}$	$\Delta\bar{\nu}$
		Band I		
a_1	594.0	16 835		
b_1	593.0	16 863		28
a_2	585.9	17 068	233	
b_2	584.2	17 117	254	49
c_2	580.7	17 221		153
a_3	578.1	17 298	230	
b_3	576.5	17 346	227	48
c_3	572.8	17 458	237	160
a_4	570.2	17 538	240	
b_4	568.7	17 584	238	46
c_4	565.4	17 687	229	149
a_5	562.8	17 768	230	
b_5	561.3	17 816	232	48
c_5	558.0	17 921	234	153
a_6	555.8	17 992	224	
b_6	554.4	18 038	222	46
c_6	551.3	18 139	218	147
a_7	549.2	18 208	216	
b_7	547.6	18 262	224	54
c_7	544.9	18 352	213	144
b_8	541.5	18 467	205	
d_1	539.9	18 522		
c_8	538.5	18 570	218	
d_2	533.9	18 730	208	
	530.3	18 857		
d_3	527.7	18 950	220	
d_4	521.6	19 172	222	
	517.5	19 324		
d_5	515.5	19 399	227	
	512.9	19 497		
d_6 (?)	510.5	19 589	190	
		Band II		
e_1	509.3	19 635		
e_2	503.9	19 845	210	
f_2	502.5	19 900		55
e_3	498.8	20 048	203	
f_3	497.3	20 109	209	61
e_4	494.0	20 245	197	
f_4	492.3	20 315	206	70
e_5	488.8	20 458	213	
f_5	487.3	20 523	208	65
g_5	485.6	20 593		135
e_6	484.0	20 663	205	
f_6	482.5	20 728	205	65
g_6	480.7	20 803	210	140
e_7	479.2	20 868	205	
f_7	477.8	20 931	203	63
g_7	476.0	21 008	205	140
e_8	474.6	21 073	205	
f_8	473.3	21 128	197	55
g_8	471.4	21 213	205	140
e_9	470.1	21 274	201	
f_9	469.0	21 324	196	50
g_9	466.8	21 422	209	148
e_{10}	465.6	21 478	204	
f_{10}	464.6	21 524	200	46
g_{10}	462.8	21 608	186	130
e_{11}	461.7	21 661	183	
f_{11}	460.5	21 716	192	55
g_{11}	458.5	21 810	202	149
e_{12}	457.3	21 867	206	
f_{12}	456.2	21 920	204	53
e_{13}	453.5	22 053	186	
f_{13}	452.3	22 109	189	56
e_{14}	449.7	22 237	184	
f_{14}	448.4	22 302	193	65
e_{15}	455.7	22 437	200	
f_{15}	444.4	22 502	200	65
e_{16}	441.9	22 632	195	
f_{16}	440.7	22 691	189	59

[a] Band position errors are estimated to be ±0.2 nm. Transitions without any assignment do not fit any of the above progressions.

---

(18) (a) Cowman, C. D.; Gray, H. B. *J. Am. Chem. Soc.* **1973**, *95*, 8177. (b) Cotton, F. A.; Martin, D. S.; Fanwick, P. E.; Peters, T. J.; Webb, T. R. *Ibid.* **1976**, *98*, 4681. (c) Cowman, C. D.; Trogler, W. C.; Gray, H. B. *Isr. J. Chem.* **1976**, *15*, 308. (d) Sattelberger, A. P.; Fackler, J. P. *J. Am. Chem. Soc.* **1977**, *99*, 1258. (e) Fanwick, P. E.; Martin, D. S.; Cotton, F. A.; Webb, T. R. *Inorg. Chem.* **1977**, *16*, 2103. (f) Martin, D. S.; Newman, R. A.; Fanwick, P. E. *Ibid.* **1979**, *18*, 2511.

somewhat poorly resolved vibrational structure was interpreted in terms of a progression frequency of ca. 400 cm^{-1} and the band assigned to a $\delta \rightarrow d_{x^2-y^2}$ ($^1A_{1u} \leftarrow {}^1A_{1g}$) transition, also orbitally forbidden. A band III was also reported as a shoulder on a strong charge-transfer absorption at shorter wavelength, centered at ca. 423 nm and with an irregular progression having a spacing of about 182 cm^{-1}. It was assigned as a $\pi \rightarrow \delta^*$ ($^1E_g \leftarrow {}^1A_{1g}$) transition. The stronger bands at higher energies were assigned as ligand-to-metal charge-transfer (LMCT) transitions.

The assignments just summarized were made on the basis of vibrational progressional frequencies, polarization data, halide-substitution-induced frequency shifts, and the nonrelativistic Xα-SW calculations of Mortola et al.[1] However, several aspects of this earlier spectroscopic study are unsatisfying, namely: (1) The spectroscopic data were said to have been measured by using the (100) face of crystals grown from acetonitrile on a quartz substrate, but it is not clear that the identification of the face was substantiated by optical crystallographic measurements. (2) Neither calculated nor observed polarization ratios were reported, a crucial omission in view of the disordered crystal structure[4] of [n-Bu$_4$N]$_2$[Re$_2$Cl$_8$]. (3) The rationale that a $\delta \rightarrow d_{x^2-y^2}$ transition, as band II has been assigned, will strengthen the Re–Cl bond is tenuous at best since elementary considerations show that there can be no unoccupied molecular orbitals that are Re–Cl σ bonding, and, in fact, the $d_{x^2-y^2}$ orbital should be Re–Cl antibonding. The principal basis for this assignment was the alleged progressional frequency of $\sim$400 cm^{-1}, higher than any fundamental frequency in the ground electronic state.[20] (4) Finally, there was only rough agreement between calculated and observed transition energies and it was not clear whether the inclusion of relativistic corrections in the Xα calculations would improve the agreement or, instead, suggest alternative assignments for the spectrum.

We addressed point 4 first. Inspection of Figure 1 and Table II indicates that shifts of up to 0.5 eV occur in the energies of molecular orbitals containing significant Re character. The shifts are not uniform in either magnitude or direction, although they generally parallel the results obtained for atoms in that MO's containing contributions only from Re 5d orbitals are destabilized while those that can include 6s or 6p character are either destabilized to a lesser degree or stabilized. These nonuniform shifts naturally have a substantial effect upon the predicted transition energies. The new predicted transition energies in Table II appear to agree quite well (within 2000 cm^{-1}) with the observed energies of the three weak bands (I, II, III) reported by TCGC. Unfortunately, the assignments given by the new calculations are *not* those proposed by TCGC! It was this inconsistency that constituted the point of departure for the new experimental studies reported here. A need for better experimental data was also implied by the considerations covered under points 1 to 3 above.

The new experimental study differs from that in TCGC in several important respects. First, crystals were grown from CH$_3$OH/HCl since we found CH$_3$CN to be unsuitable for obtaining crystals. It is noteworthy that CH$_3$OH/HCl is also the solvent from which the crystals used to determine the structure (including the extent of orientational disorder of the Re–Re bond) of [(C$_4$H$_9$)$_4$N]$_2$[Re$_2$Cl$_8$] were grown. Second, in this work great care was taken to establish the identity of the crystal face being examined. It was conclusively shown to be the (110) face in contrast to the contention of TCGC that they used the (100) face; however, this is a point to which we shall return. Third, our spectra were recorded at 5 K rather than 15 K, thereby reducing the available thermal energy by a factor of 3.

The new spectra for bands I and II are shown in Figures 2 and 3 and are tabulated in Table IV. Before discussing our new assignments of these bands, it is useful to note qualitatively the similarities and differences between our results and those previously reported by TCGC. Most striking, perhaps, is the fact that, despite the sharper definition of detail in the new spectra, they are very similar in overall appearance of those of TCGC.

Band I consists of a major progression of strong peaks as well as additional progressions of lower intensity. Peak profiles are sharper than those reported by TCGC, probably because of the lower temperature. It is now evident that these are two Franck–Condon envelopes contained in band I rather than only one, as reported previously. Band II also consists of several progressions, and again the resolution is superior to that previously available. It is important that we can now see clearly that the progressional frequency in band II is ca. 200 cm^{-1} rather than ca. 400 cm^{-1} as previously proposed. This will strongly influence the reasoning used in assigning band II. As for the previously reported and assigned band III, we have been unable to detect it. We find no evidence of a shoulder or of any vibrational structure in the spectral region 400–430 nm. Let us now look at the new experimental data for bands I and II in detail and see what support they provide for the possible assignments.

Band I. Band I consists of at least four progressions (a, b, c, and d) based on progression frequencies of 225 ± 10 cm^{-1}. In addition there are several peaks that remain unassigned. As suggested by TCGC, a progressional frequency of the magnitude 225 ± 10 cm^{-1} is almost certainly due to an excited state Re–Re stretch, thus indicating that, for the most part, these progressions are built on transitions localized in the metal–metal bonding manifold. It is also apparent, particularly in the $\|c$ spectrum, that this band contains two major envelopes, with maxima at ca. 17 600 and 18 400 cm^{-1}; these ostensibly are due to separate electronic transitions, a result not anticipated on the basis of the improved Xα calculations.

It is difficult to measure the polarization ratios accurately for progressions a, b, c, and d because of a band overlap. Progression a may be measured with the least error and, on the basis of peak heights at 555.7 nm, the measured ratio is 2.6, which agrees acceptably with the previously mentioned calculated ratio of 2.31 for a z-polarized transition. Progressions c and d are also apparently z polarized while progression b is xy polarized. These observations are in accord with those reported by TCGC. It is to be noted that accurate polarization ratio measurements for bands I and II, even if they could be obtained, would doubtless deviate from the calculated values because of the intensity borrowing mechanism by which vibronically allowed transitions occur.

We propose that both the $\pi \rightarrow \delta^*$ ($^1E_g \leftarrow {}^1A_{1g}$) and $\delta \rightarrow \pi^*$ ($^1E_g \leftarrow {}^1A_{1g}$) transitions are contained in band I. While such an assignment is somewhat at odds with the calculated splitting of $\sim$5000 cm^{-1} between these two ^1E_g states, we feel it is supported by the following considerations. According to the qualitative orbital picture of quadruply bonded metal–metal systems, these two transitions should be the lowest lying orbitally forbidden ones; moreover, each of them should weaken the Re–Re bond to about the same degree, thus accounting for the facts that nearly all of the progressional differences are 225 ± 10 cm^{-1} and the two transitions exhibit similar Franck–Condon envelopes.

We shall not attempt to provide a detailed vibronic analysis for any of the progressions in band I. Apparently, each one consists of successive quanta of the totally symmetric "Re–Re stretching" vibration in the electronic excited state, the frequency of 225 ± 10 cm^{-1} being lower by a reasonable amount than that in the ground state,[20] ca. 280 cm^{-1}. Progressions a, c, and d, which are z polarized, must couple a vibrational wave function of overall E$_u$ symmetry to the electronic wave function to give a vibronic state of A$_{2u}$ symmetry. Progression b, on the other hand, must use a nondegenerate ungerade vibration. Too little is known with certainty about the normal vibrations of the [Re$_2$Cl$_8$]$^{2-}$ ion to allow a worthwhile attempt to identify the activating vibrations in detail.

Band II. While the above assignment for band I is in at least partial agreement with that presented in TCGC, we are led to a major revision in the assignment of band II. This band is made up of three progressions, e, f, and g, each with a progressional frequency of ca. 200 cm^{-1}. This implies that it should be assigned so as to have an excited state with an Re–Re stretching frequency of about 200 cm^{-1} (the ground-state frequency[20] is about 280 cm^{-1})

---

(19) Hay, P. J. *J. Am. Chem. Soc.* **1982**, *104*, 7007.

(20) The Re–Cl stretching modes do not exceed 360 cm^{-1} according to: Oldham, C.; Ketteringham, A. P. *J. Chem. Soc., Dalton Trans.* **1973**, 2304. See also: Bratton, W. K.; Cotton, F. A.; Debeau, M.; Walton, R. A. *J. Coord. Chem.* **1971**, *1*, 121.

Table V. Summary of Spectroscopic Observations, Assignments, and Calculated Transition Energies for the Forbidden Visible Absorptions of $[n\text{-}Bu_4N]_2[Re_2Cl_8]$

approx band origin, nm (cm^{-1})	mean progressional frequency, cm^{-1} [a]		assignment[d]		calculated, cm^{-1}
	TCGC[b]	this work[c]	TCGC	this work	
600 (16 600)	222	229 (a)	$\delta \rightarrow \pi^*$ (^1E_g)	$\pi \rightarrow \delta^*$ (^1E_g)	16 730
		213 (d)		$\delta \rightarrow \pi^*$ (^1E_g)	22 120
500 (20 000)	406	200 (e)	$\delta \rightarrow d_{x^2-y^2}$ ($^1A_{1u}$)	$\pi \rightarrow \pi^*$ ($^3A_{2u}$)	28 550
440 (22 700)	182	not obsd	$\pi \rightarrow \delta^*$ (^1E_g)		

[a] Unweighted mean of the principal progression of each band. [b] TCGC: ref 3. [c] The label from Table IV of the progression used to calculate the mean is given in parentheses. [d] The final electronic state is given in parentheses.

rather than one with an enhanced Re–Cl stretching mode. We next observe that the e and f progressions appear to be *xy* polarized. Peak height measurements at 488.8 and 487.3 nm yield a polarization ratio ($\perp c/\|c$) of about 0.5 , which is in reasonable agreement with the estimate mentioned earlier of 0.64 for an *xy*-polarized transition based on the crystal structure. Progression g is too weak to permit an attempt at quantitative study, but it appears definitely to be stronger in the $\perp c$ than in the $\| c$ direction, which suggests that this progression is *z* polarized.

In assigning band II it is necessary to account for the extremely long Franck–Condon progression, the *xy* polarization of the band, the low intensity of the transition, and the marked weakening of the Re–Re bond in the excited state. For all of these reasons we favor assigning band II to the orbitally allowed, spin-forbidden $\pi \rightarrow \pi^*$ ($^3A_{2u} \leftarrow {}^1A_{1g}$) transition, which, in contrast to the singlet–singlet transition, will be *xy* polarized by virtue of its spin function. Such a transition should significantly weaken the Re–Re bond, leading to a considerably longer bond in the excited state and hence to a very long Franck–Condon progression, as observed.

The assignment of band II as a $\pi \rightarrow \pi^*$ triplet transition, while reasonable on spectroscopic and intuitive grounds, is not well corroborated by calculated energies for this transition. Our relativistic transition-state calculations place this band at $\approx$28 500 cm^{-1}, nearly 9000 cm^{-1} higher than observed. The relativistic GVB-CI calculations of Hay[19] place this transition at about 32 000 cm^{-1}; however, Hay argues for an empirical 1.4-eV downward shift of this transition energy, which leads to nearly perfect agreement ($\sim$20 900 cm^{-1}) with the assignment proposed above. The reasons for the discrepancy between the observed and calculated values of this transition are not apparent to us. The similarities and differences between the assignments presented here and those of TCGC are summarized in Table V.

Additional Observations. The suggested assignment of band II to a dipole-allowed but spin-forbidden (i.e., singlet to triplet) transition raises the interesting question of where other singlet to triplet transitions might occur not only in this case, but in the spectra of M–M quadruple bonds more generally. In all cases the lowest energy transition should be the spin-forbidden $\delta \rightarrow \delta^*$ ($^3A_{2u} \leftarrow {}^1A_{1g}$) transition. The $^3A_{2u}$ state should lie much lower than the $^1A_{2u}$ state since the singlet–triplet $\delta \rightarrow \delta^*$ transition is essentially a spin flip to give a purely covalent state whereas the singlet–singlet transition involves the "hopping" of an electron from one rhenium atom to the other, giving a primarily ionic state.[14] It is this ionic state that is primarily responsible for the inadequacy of single-configuration methods for calculating the energetics of weakly coupled electrons such as the singlet–singlet $\delta \rightarrow \delta^*$ transition energy.[14,21] This difficulty is *not* present in calculations of the singlet–triplet transition, however. Thus, we expect that the $\delta \rightarrow \delta^*$ ($^3A_{2u} \leftarrow {}^1A_{2u}$) transition in $[Re_2Cl_8]^{2-}$ should occur at the calculated energy of $\sim$3600 cm^{-1}, in the infrared. Hay[19] predicts that this transition will occur at $\sim$3200 cm^{-1}, so in this case there is essential agreement between the very disparate Xα-SW and GVB–CI approaches. Investigations are currently in progress to attempt to detect this band,[22] which will undoubtedly be quite weak.

Acknowledgment. We thank Dr. P. Jeffrey Hay for a copy of his manuscript prior to publication. This research was supported by the National Science Foundation and the Robert A. Welch Foundation.

Registry No. $Re_2Cl_8^{2-}$, 19584-24-8.

---

(21) Benard, M. *J. Chem. Phys.* **1979**, *71*, 2546.

(22) Bursten, B. E.; Sattelberger, A. P., work in progress.